PHILOSOPHICAL TRANSACTIONS OF THE ROYAL SOCIETY A MATHEMATICAL, PHYSICAL & ENGINEERING SCIENCES

# Resolving ambiguities in auto–calibration

The Royal Society

*Phil. Trans. R. Soc. Lond. A* 1998 **356**, 1193-1211
doi: 10.1098/rsta.1998.0217

The Royal Society

# Resolving ambiguities in auto-calibration

By Andrew Zisserman, David Liebowitz and Martin Armstrong

*Department of Engineering Science, University of Oxford, Parks Road, Oxford OX1 3PJ, UK*

Three-dimensional (3D) projective structure, that is structure modulo a projectivity of 3D space, can be recovered from its projection in multiple perspective images. The images might be acquired, for example, by a moving monocular camera or a stereo rig. This projective structure can be upgraded to Euclidean structure by identifying two entities, the plane at infinity and the absolute conic.

Auto-calibration methods use constraints induced by the rigid motion of the camera to determine the Euclidean structure (or equivalently the camera calibration). Often these motion constraints are supplemented by known values of the camera's internal parameters or scene constraints in order to resolve ambiguities or stabilize the algorithms.

It is shown in this paper that in certain common situations this supplementary information may not resolve the ambiguity. This is illustrated for the particular ambiguity arising for motions with a single direction of the rotation axis. Four types of constraint are analysed, and the conditions under which the ambiguity is not resolved are given. The constraint cases are: perpendicular image axes (the zero-skew constraint); specified image aspect ratio; specified image principal point; and perpendicularity of scene features.

**Keywords: camera calibration; stereo; projective geometry; reconstruction ambiguity; self-calibration**

## 1. Introduction

The auto- (or self-) calibration problem in computer vision is the following: given only corresponding features between multiple images of a scene, determine the metric structure of the scene and cameras. Generally the features are points, and auto-calibration methods proceed by first obtaining an $n$-view projective reconstruction, i.e. points $\boldsymbol{X}$ in 3-space and camera projection matrices $P$ such that

$$\boldsymbol{x}_1 = P_1\boldsymbol{X},\ \boldsymbol{x}_2 = P_2\boldsymbol{X}, \ldots, \boldsymbol{x}_n = P_n\boldsymbol{X},$$

where $\boldsymbol{x}_i$ is the measured image point, and $P_i$ the camera, for the $i$th view. At this stage $\boldsymbol{X}$ and $P$ are only determined up to a common, but unknown, projective transformation (homography) of 3-space. The three-dimensional (3D) structure and cameras are then 'upgraded' to metric by either implicitly or explicitly identifying the plane at infinity and the absolute conic. There are three types of constraint which are available for this upgrade:

1. motion based, e.g. that the motion is a Euclidean transformation of 3-space;

2. structure based, e.g. that scene lines are parallel or orthogonal;

3. internal based, e.g. that the camera's internal parameters are constant or have particular values.

Research in auto-calibration originated with the paper of Faugeras *et al.* (1992) where the Kruppa constraints on the fixed internal parameters were obtained from the fundamental matrix. Since then several investigative trends have emerged: the first trend is for exact or closed form solutions for the polynomial constraints arising from view pairs (Luong 1992; Hartley 1992; Pollefeys *et al.* 1996; Bougnoux 1998) using the fundamental matrix, or view triplets using the trifocal tensor (Armstrong *et al.* 1996); a second trend is for the numerical minimization of suitable measures for an over-constrained system (Hartley 1994*a*; Pollefeys *et al.* 1998; Triggs 1997; Zeller 1996); and a third for existence proofs (Heyden & Åström 1997; Pollefeys *et al.* 1998). Auto-calibration algorithms have also been developed for special motions of monocular cameras (Armstrong *et al.* 1994, 1996; Hartley 1994*b*) and stereo rigs (Beardsley & Zisserman 1995; Devernay & Faugeras 1996; Horaud & Csurka 1998; Zisserman *et al.* 1995).

Currently the most successful schemes (Pollefeys *et al.* 1998) combine several of the elements above. They are formulated in terms of the dual of the absolute conic, which is a particularly concise parametrization introduced by Triggs (1997). The algorithms require a set of consistent camera matrices for the image sequence which can be obtained as described in Laveau (1996) and Beardsley *et al.* (1996). Solutions are obtained by a numerical minimization, with *a priori* information on the internal parameters included as constraints. The minimization is initialized from a linear solution to a subset of the constraints. This generation of algorithms converges reliably, is accurate, and applies to general camera motions even when some of the internal parameters are varying.

However, in certain common situations motion-induced constraints are not sufficient to determine the camera calibration. This has been pointed out by a number of authors (Zisserman *et al.* 1995; Triggs 1997), for example in the case of planar motion (where the camera rotation axis has a fixed direction, and the translation is perpendicular to this direction). These 'critical motion sequences' have been catalogued by Sturm (1997), including both continuous and discrete motions. It is generally supposed that these ambiguities are resolved once additional information is supplied, such as the value of particular internal parameters. It is shown in this paper that supplementary information may *not* resolve the ambiguity.

The particular ambiguity arising when the rotation axes are parallel for multiple camera motions is described in § 3. Section 4 provides examples of auto-calibration algorithms where this ambiguity is available in closed form. In § 5 we analyse four types of constraint and give the conditions under which the ambiguity is not resolved. The cases are: perpendicular image axes (the zero-skew constraint); specified image aspect ratio; specified image principal point; and, perpendicularity of scene features.

## 2. Background and notation

This section is a summary of the classical projective geometry notions of the plane at infinity and absolute conic, and their relationship to camera calibration. It draws on material from Faugeras (1993, 1995), Hartley (1994*b*), Kanatani (1992), Mundy & Zisserman (1992), and Semple & Kneebone (1979). The absolute conic and its image

allow the constraints arising in auto-calibration to be visualized geometrically. This section also introduces the notation for the paper.

(i) *Points, lines, and directions*

On the image plane points are represented by homogeneous 3-vectors $\boldsymbol{x}$, and lines by homogeneous 3-vectors $\boldsymbol{l}$. If a point $\boldsymbol{x}$ is on a line $\boldsymbol{l}$, then $\boldsymbol{l} \cdot \boldsymbol{x} = 0$.

In 3-space points are represented by homogeneous 4-vectors $\boldsymbol{X}$, and planes by homogeneous 4-vectors $\boldsymbol{\pi}$. Directions are points on the plane at infinity (see below) and are represented by points with $X_4 = 0$. Often only the first 3-vector component $\boldsymbol{d}$ of a direction $\boldsymbol{D}^{\mathrm{T}} = (\boldsymbol{d}^{\mathrm{T}}, 0)$ is used. In general '=' indicates equality only up to scale between homogeneous quantities.

(ii) *Conics and dual conics*

A point conic is represented by a $3 \times 3$ matrix $C$. A point $\boldsymbol{x}$ on the conic satisfies $\boldsymbol{x}^{\mathrm{T}} C \boldsymbol{x} = 0$. A dual (or line) conic is represented by a $3 \times 3$ matrix $C^*$. A line $\boldsymbol{l}$ tangent to the conic $C$ satisfies $\boldsymbol{l}^{\mathrm{T}} C^* \boldsymbol{l} = 0$. Provided $C$ is full rank $C^* = C^{-1}$, and $(C^*)^* = C$. Under a point homography $\boldsymbol{x}' = H\boldsymbol{x}$, a conic and a dual conic transform as

$$C' = H^{-\mathrm{T}} C H^{-1}, \qquad C'^* = H C^* H^{\mathrm{T}}. \tag{2.1}$$

(iii) *The plane at infinity $\boldsymbol{\pi}_\infty$ and absolute conic $\boldsymbol{\Omega}_\infty$*

The plane at infinity $\boldsymbol{\pi}_\infty$ is the plane $X_4 = 0$ in an affine frame. Parallel lines intersect on $\boldsymbol{\pi}_\infty$, and $\boldsymbol{\pi}_\infty$ is fixed (setwise) under Euclidean motions.

The absolute conic $\boldsymbol{\Omega}_\infty$ is a point conic on $\boldsymbol{\pi}_\infty$ defined as $X_1^2 + X_2^2 + X_3^2 = 0$, $X_4 = 0$. It contains only imaginary points. If points on $\boldsymbol{\pi}_\infty$ are written as $\boldsymbol{X}_\infty^{\mathrm{T}} = (\boldsymbol{x}_\infty^{\mathrm{T}}, 0)$, then $\boldsymbol{\Omega}_\infty$ is the conic $\boldsymbol{x}_\infty^{\mathrm{T}} I \boldsymbol{x}_\infty = 0$, i.e. the matrix of $\boldsymbol{\Omega}_\infty$ is the identity $I$. The conic $\boldsymbol{\Omega}_\infty$ is fixed (setwise) under Euclidean motions.

(iv) *Camera projection matrices*

Points in 3-space are mapped perspectively to points on the image by a $3 \times 4$ rank 3 camera projection matrix $P$, as $\boldsymbol{x} = P\boldsymbol{X}$. The matrix $P$ may be decomposed as $P = A[R \mid \boldsymbol{t}]$, where $R$ is a $3 \times 3$ rotation matrix, $\boldsymbol{t}$ is a translation 3-vector, and $A$ is the camera calibration matrix. The rotation $R$ and translation $\boldsymbol{t}$ represent the Euclidean transformation between the camera and world coordinate systems. The $3 \times 3$ matrix $A$ is upper triangular, and represents the internal parameters of the camera. It has the following form:

$$A = \begin{pmatrix} \alpha_u & k & u_0 \\ 0 & \alpha_v & v_0 \\ 0 & 0 & 1 \end{pmatrix}.$$

The elements $\alpha_u$ and $\alpha_v$ depend on the focal length of the camera and image axes scalings. The aspect ratio is $r = \alpha_u / \alpha_v$. The principal point is $(u_0, v_0)^{\mathrm{T}}$, and the 'skew' element $k$ depends on the physical angle between the $x$ and $y$ axes of the sensor array.

(v) *Vanishing points and lines*

Under projection by the matrix $P = A[R \mid \boldsymbol{t}]$ points on $\boldsymbol{\pi}_\infty$ are imaged as

$$\boldsymbol{x} = A[R \mid \boldsymbol{t}] \begin{pmatrix} \boldsymbol{x}_\infty \\ 0 \end{pmatrix} = AR\boldsymbol{x}_\infty, \tag{2.2}$$

which is a planar homography $\boldsymbol{x} = H\boldsymbol{x}_\infty$ between $\boldsymbol{\pi}_\infty$ and the image plane with $H = AR$. This homography is the map between directions and their vanishing points, i.e. parallel lines intersect at a point on $\boldsymbol{\pi}_\infty$, and the image of this point is a vanishing point. Note that $H$ is independent of the translation. Similarly parallel planes intersect in a line on $\boldsymbol{\pi}_\infty$, and the image of this line is the vanishing line of the planes.

(vi) *The image of the absolute conic*

The image of the absolute conic (IAC), $\boldsymbol{\omega}$, depends only on the $A$ matrix of $P$. This important result will now be derived. The mapping between $\boldsymbol{\pi}_\infty$ and the image is the planar homography (2.2) $H = AR$, and under a point homography $\boldsymbol{x} \rightarrow H\boldsymbol{x}$ a conic $C$ maps as $C \rightarrow H^{-\mathrm{T}}CH^{-1}$. It follows that $\boldsymbol{\Omega}_\infty$, which is the conic $C = \boldsymbol{\Omega}_\infty = I$ maps to $\boldsymbol{\omega} = (AR)^{-\mathrm{T}}I(AR)^{-1} = A^{-\mathrm{T}}RR^{-1}A^{-1} = (AA^{\mathrm{T}})^{-1}$. So the IAC $\boldsymbol{\omega} = (AA^{\mathrm{T}})^{-1}$, and this defines the dual image of the absolute conic (DIAC) as $\boldsymbol{\omega}^* = \boldsymbol{\omega}^{-1} = AA^{\mathrm{T}}$. This result demonstrates that once $\boldsymbol{\omega}$ (or equivalently $\boldsymbol{\omega}^*$) is determined, so is the calibration matrix $A$.

### (*a*) *Orthogonality and polarity*

We now give a geometric representation of orthogonality in a projective space based on the absolute conic and its image. The main device will be the pole–polar relationship between a point and line induced by a conic. In the following the camera coordinate system will generally be used for the world coordinates, so that $R = I$ and $\boldsymbol{t} = \boldsymbol{0}$. In this case the vanishing point of the direction $\boldsymbol{d}$ is simply $\boldsymbol{v} = A\boldsymbol{d}$.

(vii) *Pole–polar relationship*

The point $\boldsymbol{x}$ and conic $C$ define a line $\boldsymbol{l} = C\boldsymbol{x}$. The line $\boldsymbol{l}$ is the *polar* of $\boldsymbol{x}$ w.r.t. $C$, and the point $\boldsymbol{x}$ is the *pole* of $\boldsymbol{l}$ w.r.t. $C$. This relationship is illustrated in figure 1. If the point $\boldsymbol{y}$ is on the line $\boldsymbol{l}$, then $\boldsymbol{y}^{\mathrm{T}}\boldsymbol{l} = \boldsymbol{y}^{\mathrm{T}}C\boldsymbol{x} = 0$. Any two points $\boldsymbol{x}, \boldsymbol{y}$ satisfying $\boldsymbol{y}^{\mathrm{T}}C\boldsymbol{x} = 0$ are *conjugate* w.r.t. the conic $C$. The pole–polar relation is symmetric: if $\boldsymbol{x}$ is on the polar of $\boldsymbol{y}$ then $\boldsymbol{y}$ is on the polar of $\boldsymbol{x}$.

(viii) *Orthogonality in 3-space and in the image*

In 3-space directions $\boldsymbol{d}_1$ and $\boldsymbol{d}_2$ are orthogonal if $\boldsymbol{d}_1^{\mathrm{T}}\boldsymbol{\Omega}_\infty\boldsymbol{d}_2 = 0$. This result follows directly from the scalar product of two orthogonal vectors: in a Euclidean frame $\boldsymbol{d}_1^{\mathrm{T}}\boldsymbol{\Omega}_\infty\boldsymbol{d}_2 = \boldsymbol{d}_1^{\mathrm{T}}I\boldsymbol{d}_2 = \boldsymbol{d}_1^{\mathrm{T}}\boldsymbol{d}_2 = 0$. Orthogonality is thereby encoded by conjugacy. The great advantage of this is that conjugacy is a projective relation, so that in a projective frame (obtained by a projective transformation of 3-space) directions can be identified as orthogonal if they are conjugate w.r.t. $\boldsymbol{\Omega}_\infty$ in that frame (in general the matrix of $\boldsymbol{\Omega}_\infty$ is not $I$ in a projective frame). The geometric representation of orthogonality is shown in figure 2*a*.

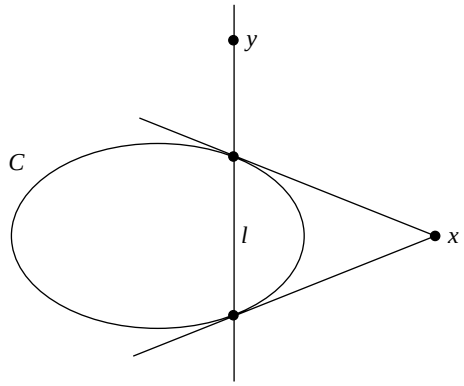


Figure 1. The pole–polar relationship. The line $\boldsymbol{l} = C\boldsymbol{x}$ is the *polar* of the point $\boldsymbol{x}$ w.r.t. the conic $C$, and the point $\boldsymbol{x} = C^{-1}\boldsymbol{l}$ is the *pole* of $\boldsymbol{l}$ w.r.t. $C$. The polar of $\boldsymbol{x}$ intersects the conic at the points of tangency of lines from $\boldsymbol{x}$. If $\boldsymbol{y}$ is on $\boldsymbol{l}$, then $\boldsymbol{y}^{\mathrm{T}}\boldsymbol{l} = \boldsymbol{y}^{\mathrm{T}}C\boldsymbol{x} = 0$. Points $\boldsymbol{x}$ and $\boldsymbol{y}$ which satisfy $\boldsymbol{y}^{\mathrm{T}}C\boldsymbol{x} = 0$ are *conjugate*.

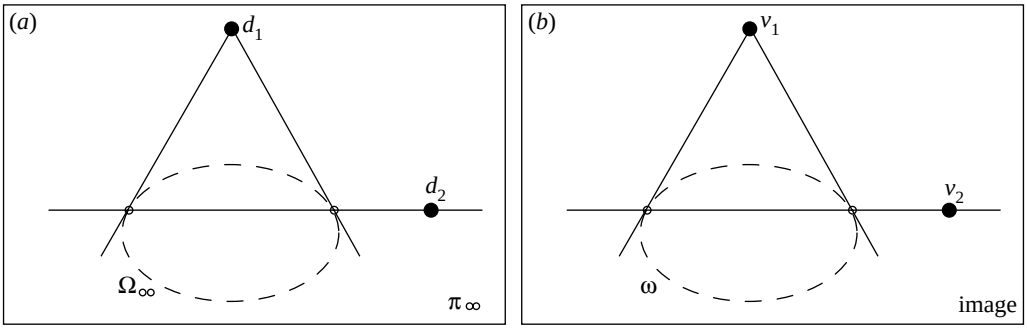


Figure 2. Orthogonality represented by the pole–polar relationship. (*a*) On $\boldsymbol{\pi}_\infty$ orthogonal directions $\boldsymbol{d}_1$, $\boldsymbol{d}_2$ are conjugate w.r.t. $\boldsymbol{\Omega}_\infty$. (*b*) On the image plane orthogonal rays $\boldsymbol{v}_1$, $\boldsymbol{v}_2$ are conjugate w.r.t. $\boldsymbol{\omega}$.

Similarly, in the image (figure 2*b*) $\boldsymbol{\omega}$ defines orthogonality: two ray directions are orthogonal if they are conjugate points w.r.t. $\boldsymbol{\omega}$, and a ray direction and plane (through the camera centre) are orthogonal if the corresponding point and line are pole–polar w.r.t. $\boldsymbol{\omega}$. These projective representations of orthogonality in the image follow directly from the projective mapping between $\boldsymbol{\pi}_\infty$ and the image: a pole–polar relationship on $\boldsymbol{\pi}_\infty$ is mapped to a pole–polar relationship on the image. In the image the scalar product between two ray directions is $\boldsymbol{d}_1 \cdot \boldsymbol{d}_2 = (A^{-1}\boldsymbol{v}_1) \cdot (A^{-1}\boldsymbol{v}_2) = \boldsymbol{v}_1^{\mathrm{T}}A^{-\top}A^{-1}\boldsymbol{v}_2 = \boldsymbol{v}_1^{\mathrm{T}}\boldsymbol{\omega}\boldsymbol{v}_2$. So, if $\boldsymbol{v}_1^{\mathrm{T}}\boldsymbol{\omega}\boldsymbol{v}_2 = 0$, then the directions $\boldsymbol{d}_1, \boldsymbol{d}_2$ are orthogonal.

### (ix) *Vanishing points and lines*

The vanishing point of lines with direction $\boldsymbol{d}$ in 3-space is the intersection $\boldsymbol{v}$ of the image plane with a ray through the camera centre with direction $\boldsymbol{d}$, namely $\boldsymbol{v} = A\boldsymbol{d}$. Similarly, the vanishing line of planes perpendicular to the direction $\boldsymbol{d}$ in 3-space is the intersection $\boldsymbol{l}$ of a plane through the camera centre perpendicular to $\boldsymbol{d}$, that is $\boldsymbol{l} = A^{-\mathrm{T}}\boldsymbol{d}$.

Consider a vanishing point $\boldsymbol{v}$, its polar, $\boldsymbol{l} = \boldsymbol{\omega v} = (AA^{\mathrm{T}})^{-1}A\boldsymbol{d} = A^{-\mathrm{T}}\boldsymbol{d}$, is the vanishing line of planes perpendicular to the direction $\boldsymbol{v}$. Similarly, the pole of a line $\boldsymbol{l}$, given by $\boldsymbol{v} = \boldsymbol{\omega}^{-1}\boldsymbol{l} = \boldsymbol{\omega}^{*}\boldsymbol{l}$, is the vanishing point of the normal direction to planes with vanishing line $\boldsymbol{l}$. To summarize (all relations on vanishing points $\boldsymbol{v}$ and lines $\boldsymbol{l}$):

1. Perpendicular directions
$$\boldsymbol{v}_1^{\mathrm{T}}\boldsymbol{\omega v}_2 = 0. \tag{2.3}$$
2. Normal to plane $\boldsymbol{l} = \boldsymbol{\omega v}$.
3. Perpendicular planes $\boldsymbol{l}_1^{\mathrm{T}}\boldsymbol{\omega}^{*}\boldsymbol{l}_2 = 0$.

## 3. The ambiguity from rotations with parallel axes

Here we describe the fundamental one-parameter family ambiguity that will be examined in the rest of the paper. This ambiguity arises when the camera rotations are about axes with a common direction. Examples of algorithms for recovering the family of solutions, and the fixed points and lines discussed below, are given in § 4.

### (*a*) *The ambiguity in determining* $\boldsymbol{\Omega}_\infty$

The absolute conic may be identified as the conic on $\boldsymbol{\pi}_\infty$ fixed under any Euclidean motion. However, as will be demonstrated below, for a particular rotation axis direction a one-parameter family of conics is fixed. Suppose the camera undergoes a series of Euclidean motions with rotation axes restricted to be parallel to a fixed direction. Then attempts to identify $\boldsymbol{\Omega}_\infty$ as the conic on $\boldsymbol{\pi}_\infty$ fixed under these motions will not determine a unique conic, but only a one-parameter family of conics.

Algebraically, the Euclidean transformation (a general screw motion) can be represented without loss of generality as a $4 \times 4$ homogeneous matrix
$$H_{\mathrm{E}} = \begin{bmatrix} R & \boldsymbol{t} \\ \boldsymbol{0}^{\top} & 1 \end{bmatrix}. \tag{3.1}$$
Let $\boldsymbol{d}_{\mathrm{r}}$ be the (unit norm) direction of the rotation axis, so that $R\boldsymbol{d}_{\mathrm{r}} = \boldsymbol{d}_{\mathrm{r}}$. Under the transformation $H_{\mathrm{E}}$, points on $\boldsymbol{\pi}_\infty$ (i.e. with $X_4 = 0$) are mapped to points on $\boldsymbol{\pi}_\infty$ by the $3 \times 3$ homography $\boldsymbol{x}_\infty \rightarrow R\boldsymbol{x}_\infty$. Under this point transformation a conic on $\boldsymbol{\pi}_\infty$ maps as (2.1) $C \rightarrow R^{-\mathrm{T}}CR^{-1} = RCR^{\mathrm{T}}$.

We now examine the fixed conics under this mapping. The absolute conic $\boldsymbol{\Omega}_\infty$ is fixed since $RIR^{\mathrm{T}} = I$. However, the (degenerate) point conic $\boldsymbol{d}_{\mathrm{r}}\boldsymbol{d}_{\mathrm{r}}^{\mathrm{T}}$ is also fixed.† It follows that the one-parameter family of conics (a *pencil*)
$$C_\infty(\mu) = I + \mu\boldsymbol{d}_{\mathrm{r}}\boldsymbol{d}_{\mathrm{r}}^{\mathrm{T}} \tag{3.2}$$
is fixed under the mapping since
$$\begin{aligned} R(\boldsymbol{\Omega}_\infty + \mu\boldsymbol{d}_{\mathrm{r}}\boldsymbol{d}_{\mathrm{r}}^{\mathrm{T}})R^{\mathrm{T}} &= RIR^{\mathrm{T}} + \mu R\boldsymbol{d}_{\mathrm{r}}\boldsymbol{d}_{\mathrm{r}}^{\mathrm{T}}R^{\mathrm{T}} \\ &= \boldsymbol{\Omega}_\infty + \mu\boldsymbol{d}_{\mathrm{r}}\boldsymbol{d}_{\mathrm{r}}^{\mathrm{T}}. \end{aligned}$$
The scalar $\mu$ parametrizes the pencil. The pencil of conics $C_\infty(\mu)$ is the one-parameter family of solutions to any auto-calibration algorithm based on constraints induced by these motions.

† $\boldsymbol{d}_{\mathrm{r}}$ is here interpreted as a *line* $\boldsymbol{L}_{\mathrm{r}} = \boldsymbol{\Omega}_\infty\boldsymbol{d}_{\mathrm{r}}$, which is polar to $\boldsymbol{d}_{\mathrm{r}}$. However, since $\boldsymbol{\Omega}_\infty = I$, it follows that $\boldsymbol{L}_{\mathrm{r}} = \boldsymbol{d}_{\mathrm{r}}$.

### (*b*) *Fixed points and lines on* $\boldsymbol{\pi}_\infty$

In the following it is convenient to express the family $C_\infty(\mu)$ (3.2) in terms of the points and lines on $\boldsymbol{\pi}_\infty$ which are fixed under the motion. The fixed elements of the motion are obtained algebraically from the eigenvectors of $H_\mathrm{E}$. As described in Zisserman *et al*. (1995), the fixed points on $\boldsymbol{\pi}_\infty$ are the direction of the rotation axis $\boldsymbol{d}_\mathrm{r}$, and the circular points $\boldsymbol{I}$ and $\boldsymbol{J}$ of the planes perpendicular to the rotation axis.

The line of intersection $\boldsymbol{L}_\mathrm{r}$ of $\boldsymbol{\pi}_\infty$ with the family of planes orthogonal to the rotation axis is also fixed (setwise). The line $\boldsymbol{L}_\mathrm{r}$ intersects $\boldsymbol{\Omega}_\infty$ in the circular points $\boldsymbol{I}$ and $\boldsymbol{J}$. The point $\boldsymbol{d}_\mathrm{r}$ and line $\boldsymbol{L}_\mathrm{r}$ correspond to a direction and family of planes, respectively, which are orthogonal. Consequently, $\boldsymbol{d}_\mathrm{r}$ and $\boldsymbol{L}_\mathrm{r}$ are pole–polar w.r.t. $\boldsymbol{\Omega}_\infty$.

These relations between the fixed points and lines and $\boldsymbol{\Omega}_\infty$ determine $\boldsymbol{\Omega}_\infty$ up to the one-parameter family (3.2). To avoid repetition this family and its parametrizations will not be described here, but instead will be described in the following section for the fixed points and lines in the image, and their relation to $\boldsymbol{\omega}$. The same relations apply in both cases.

### (*c*) *The ambiguity in determining* $\boldsymbol{\omega}$

If it is further supposed that under the motion the camera's internal parameters $A$ are fixed, then the IAC is also fixed, as are the images of the other fixed entities on $\boldsymbol{\pi}_\infty$. The constraints on $\boldsymbol{\omega}$ arising from the imaged fixed points are:

1. The imaged circular points, $\boldsymbol{c}_i$, $\boldsymbol{c}_j$ are on $\boldsymbol{\omega}$, i.e. $\boldsymbol{c}_i^\mathrm{T}\boldsymbol{\omega}\boldsymbol{c}_i = 0$, $\boldsymbol{c}_j^\mathrm{T}\boldsymbol{\omega}\boldsymbol{c}_j = 0$. These are two constraints on $\boldsymbol{\omega}$.

2. There is a pole–polar relation on $\boldsymbol{\omega}$ between the line through the imaged circular points, $\boldsymbol{l}_\mathrm{r} = \boldsymbol{c}_i \times \boldsymbol{c}_j$, and the vanishing point of the rotation axis direction $\boldsymbol{v}_\mathrm{r}$, i.e. $\boldsymbol{\omega}\boldsymbol{v}_\mathrm{r} = \boldsymbol{l}_\mathrm{r}$. These are two constraints on $\boldsymbol{\omega}$.

These relations are illustrated in figure 3*a*. The lines $\boldsymbol{l}_i, \boldsymbol{l}_j$, which are tangent to $\boldsymbol{\omega}$, are defined as $\boldsymbol{l}_i = \boldsymbol{v}_\mathrm{r} \times \boldsymbol{c}_i$ and $\boldsymbol{l}_j = \boldsymbol{v}_\mathrm{r} \times \boldsymbol{c}_j$.

There are a total of four constraints on the five degrees of freedom of $\boldsymbol{\omega}$, and consequently a pencil of conics $C(\mu)$ satisfies these constraints. The pencil is illustrated in figure 3*b*. This family of solutions is simply the mapping of the pencil (3.2) onto the image plane. The projective relations of intersection and pole–polarity between $\boldsymbol{\Omega}_\infty$ and the fixed points and lines on $\boldsymbol{\pi}_\infty$ are preserved under the mapping. The mapping is by the matrix $A$, and under this point homography $C(\mu) = A^{-\top}C_\infty(\mu)A^{-1} = A^{-\top}(I + \mu\boldsymbol{d}_\mathrm{r}\boldsymbol{d}_\mathrm{r}^\mathrm{T})A^{-1} = \boldsymbol{\omega} + \mu\boldsymbol{l}_\mathrm{r}\boldsymbol{l}_\mathrm{r}^\mathrm{T}$.

This pencil can be represented by the linear combination of any two conics within it (Semple & Kneebone 1979). In particular the conics can be degenerate. It follows that the pencil may be written as

$$C(\mu) = \boldsymbol{\Lambda}_2 + \mu\boldsymbol{\Lambda}_1 = (\boldsymbol{l}_i\boldsymbol{l}_j^\mathrm{T} + \boldsymbol{l}_j\boldsymbol{l}_i^\mathrm{T}) + \mu(\boldsymbol{l}_\mathrm{r}\boldsymbol{l}_\mathrm{r}^\mathrm{T}), \tag{3.3}$$

where $\mu$ parametrizes the family. The conic $\boldsymbol{\Lambda}_1$ is rank 1, and $\boldsymbol{\Lambda}_2$ is rank 2.

Both the degenerate conics $\boldsymbol{\Lambda}_1$ and $\boldsymbol{\Lambda}_2$ are specified entirely in terms of fixed points and lines which can be obtained from image measurements (via the methods of § 4). This is preferable to the $C(\mu) = \boldsymbol{\omega} + \mu\boldsymbol{\Lambda}_1$ parametrization above which involves the (unknown) image of the absolute conic. The pencil can also be written

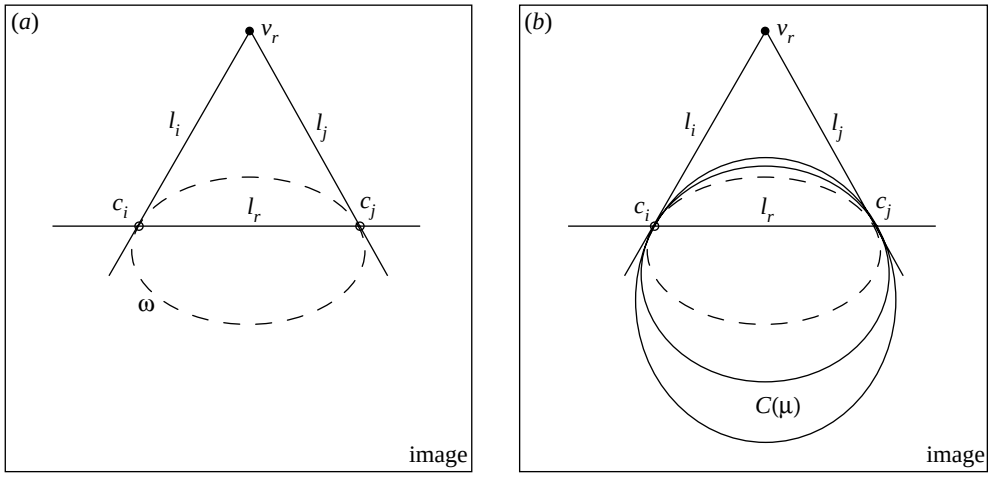


Figure 3. (*a*) The image fixed points and lines under a rotation, and their relation to $\boldsymbol{\omega}$. The point $\boldsymbol{v}_\mathrm{r}$ is the vanishing point of the rotation axis direction, and $\boldsymbol{c}_i$ and $\boldsymbol{c}_j$ are the imaged circular points for planes orthogonal to the rotation axis. The line $\boldsymbol{l}_\mathrm{r}$ is the vanishing line for planes orthogonal to the rotation axis. The image of the absolute conic contains the imaged circular points. The point $\boldsymbol{v}_\mathrm{r}$ and line $\boldsymbol{l}_\mathrm{r}$ have a pole–polar relationship w.r.t. $\boldsymbol{\omega}$; with $\boldsymbol{\omega}$ tangent to the lines $\boldsymbol{l}_i, \boldsymbol{l}_j$ at the imaged circular points. (*b*) These relations do not uniquely define the conic $\boldsymbol{\omega}$. There is a pencil of conics $C(\mu)$ consistent with the constraints.

as $C(\mu) = \boldsymbol{\omega} + \mu\boldsymbol{\Lambda}_2$, again involving the unknown $\boldsymbol{\omega}$. Note, $\mu$ parametrizes all point conic pencils. However, the same value of $\mu$ will not generate the same conic from each family.

### (*d*) *The ambiguity arising from the infinite homography*

The infinite homography $H_\infty$, which was introduced by Luong & Viéville (1994), is the point homography between image planes induced by the plane at infinity. If the camera undergoes a rotation $R$ and a translation $\boldsymbol{t}$, then vanishing points map between images as $\boldsymbol{v} \rightarrow H_\infty \boldsymbol{v}$. The infinite homography depends only on the rotation between views and the internal parameters, and is given by $H_\infty = ARA^{-1}$. The infinite homography is of interest here because the fixed points and lines under the mapping $H_\infty$ determine the images of fixed points and lines on $\boldsymbol{\pi}_\infty$.

Suppose $H_\infty$ is known. Then the IAC (and DIAC) may be determined up to the one-parameter family (3.3) above. Luong & Viéville (1996) originally showed that the DIAC could be determined in this manner. Here a derivation is given for the IAC and the relationship to the eigenvectors of $H_\infty$ established.

#### (i) *Geometric solution*

The infinite homography is represented by a $3 \times 3$ matrix $H_\infty$. The eigenvectors of this matrix are the fixed points, and the eigenvectors of $H_\infty^\mathrm{T}$ are the fixed lines. The matrix $H_\infty = ARA^{-1}$ has an eigenvector $\boldsymbol{v}_\mathrm{r} = A\boldsymbol{d}_\mathrm{r}$ with unit eigenvalue. The three eigenvectors of $H_\infty$ have the following geometric interpretation:

1. $\boldsymbol{v}_\mathrm{r}$, corresponding to the unit eigenvalue, is the vanishing point of the rotation axis.

2. $\boldsymbol{c}_i$ and $\boldsymbol{c}_j$, corresponding to the eigenvalues $\mathrm{e}^{\pm \mathrm{i}\theta}$, are the images of the circular points of planes orthogonal to the rotation axis.

Similarly, the eigenvectors of $H_\infty^{\mathrm{T}}$ are

1. $\boldsymbol{l}_{\mathrm{r}}$, corresponding to the unit eigenvalue, is the vanishing line of planes orthogonal to the rotation axis.

2. $\boldsymbol{l}_i$ and $\boldsymbol{l}_j$, corresponding to the eigenvalues $\mathrm{e}^{\pm \mathrm{i}\theta}$, are lines through $\boldsymbol{v}_{\mathrm{r}}$ and each of the circular points.

The eigenvalue angle $\theta$ is the (Euclidean) angle of rotation about the axis. These fixed points and lines and their relation to the IAC are again those of figure 3, and the pencil of solutions (3.3) for $\boldsymbol{\omega}$ can be written directly from these eigenvectors.

(ii) *Algebraic solution*

Using the transformation properties of conics under a homography (2.1) for point and dual conics, the constraint that $\boldsymbol{\omega}$ (and $\boldsymbol{\omega}^*$) are fixed under the $H_\infty$ mapping becomes

$$\boldsymbol{\omega} = H_\infty^{\mathrm{T}} \boldsymbol{\omega} H_\infty \tag{3.4}$$

and $\boldsymbol{\omega}^* = H_\infty \boldsymbol{\omega}^* H_\infty^{\mathrm{T}}$.

Here we will give the solution for (3.4); the solution for $\boldsymbol{\omega}^*$ is analogous. The scale factor in the homogeneous equation can be chosen as unity provided $H_\infty$ is normalized as $\det H_\infty = 1$. Equation (3.4) can then be written in a homogeneous *linear* form $M\boldsymbol{c} = \boldsymbol{0}$, where $M$ is a $6 \times 6$ matrix composed from the elements of $H_\infty$, and $\boldsymbol{c}$ is the conic $\boldsymbol{\omega}$ written as a 6-vector. It can be shown that $M$ is at most rank 4, so that there is a one-parameter family of (homogeneous) solutions for $\boldsymbol{c}$,

$$\boldsymbol{c}(\mu) = \boldsymbol{n}_1 + \mu \boldsymbol{n}_2,$$

where $\boldsymbol{n}_i$ span the two-dimensional nullspace of $M$. The matrix family is then obtained as $C(\mu) = N_1 + \mu N_2$, where $N_1, N_2$ are the matrices corresponding to $\boldsymbol{n}_1, \boldsymbol{n}_2$, respectively. This family is identical to the family $C(\mu)$ (3.3) given by any of the three parametrizations in terms of $\boldsymbol{\Lambda}_1$ and $\boldsymbol{\Lambda}_2$. For example, if $\boldsymbol{\omega}$ is a solution to $\boldsymbol{\omega} = H_\infty^{\mathrm{T}} \boldsymbol{\omega} H_\infty$, then so is $C(\mu) = \boldsymbol{\omega} + \mu \boldsymbol{l}_{\mathrm{r}} \boldsymbol{l}_{\mathrm{r}}^{\mathrm{T}}$ (i.e. $H_\infty^{\mathrm{T}} C(\mu) H_\infty = C(\mu)$).

The form of the one-parameter family for $\boldsymbol{\omega}^*$ follows in a similar manner. For example, if $\boldsymbol{\omega}^*$ is a solution to $\boldsymbol{\omega}^* = H_\infty \boldsymbol{\omega}^* H_\infty^{\mathrm{T}}$, then so is $C^*(\lambda) = \boldsymbol{\omega}^* + \lambda \boldsymbol{v}_{\mathrm{r}} \boldsymbol{v}_{\mathrm{r}}^{\mathrm{T}}$.

Insight into ambiguities which can be resolved for particular rotations can be obtained directly by considering the form of $H_\infty$ (Armstrong *et al*. 1994). For example, for a rotation parallel to the image $x$ axis, $H_\infty = A R_{\mathrm{X}} A^{-1}$. When $k = 0$, as is usual, there are no terms involving $\alpha_u$ in $H_\infty$, so there are no possible constraints on $\alpha_u$ in (3.4). Consequently, the pencil will not have the veridical value of $\alpha_u$, and a constraint that supplies the veridical value will resolve the ambiguity. Similarly, for a rotation parallel to the image $y$ axis, $\alpha_v$ is unconstrained, and for a rotation perpendicular to the image plane $\alpha_u$ and $\alpha_v$ only occur as the ratio $\alpha_u/\alpha_v$, so their individual values are unconstrained.

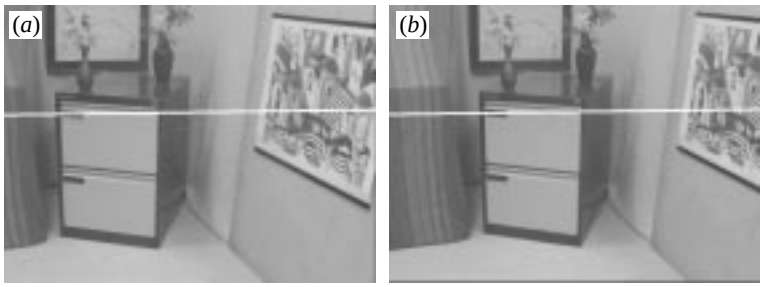


Figure 4. The motion between ($a$) and ($b$) is a rotation about the camera centre, with the rotation axis approximately parallel to the image $y$-axis. The white line is the fixed line $\boldsymbol{l}_{\mathrm{r}}$ computed from the eigenvectors of $H_\infty$.

## 4. Where do one-parameter families arise?

This section reviews four methods that have been developed to identify the plane at infinity and the absolute conic from multiple images. For each of the methods:

1. The camera undergoes a single motion, or multiple motions with rotations about parallel axes.

2. The internal parameters $A$ are fixed during the motion.

3. The algorithms provide a method for accessing the vanishing point of the rotation axis and the imaged circular points.

### ($a$) *Single rotation of a camera about its centre*

If there is a pure rotation about the camera centre, then, as shown by Hartley (1994*b*), $H_\infty$ can be computed directly from the homography between the images. The eigenvectors of $H_\infty$ are $\boldsymbol{v}_{\mathrm{r}}, \boldsymbol{c}_i$ and $\boldsymbol{c}_j$, from which the three lines composing the degenerate conics (3.3) are obtained directly. Figures 4 and 5 show examples of the fixed point $\boldsymbol{v}_{\mathrm{r}}$ and fixed line $\boldsymbol{l}_{\mathrm{r}} = \boldsymbol{c}_i \times \boldsymbol{c}_j$, computed from the eigenvectors of $H_\infty$, which is determined from the homography between the images.

### ($b$) *Planar motion of a monocular camera*

Suppose a camera undergoes planar motion, then the fixed points and lines over the sequence are those of figure 3. The trifocal tensor provides a mapping between corresponding lines over three views, i.e. if $\boldsymbol{l}$, $\boldsymbol{l}'$ and $\boldsymbol{l}''$ are the images of the same line in three views, then $l_i = l'_j l''_k T_i^{jk}$ (Hartley 1995), where $T_i^{jk}$ is the trifocal tensor for the three views. The fixed image lines are obtained as fixed line solutions $\boldsymbol{l}$ to this mapping, i.e. $l_i = l_j l_k T_i^{jk}$.

In Armstrong *et al*. (1996) an algorithm is described whereby the fixed lines are obtained from a cubic in one variable derived from the trifocal tensor. The tensor is computed automatically from point (image corner) correspondences over three views. Armstrong (1996) shows that improved results are obtained by bundle-adjustment over a sequence consisting of more than three views.

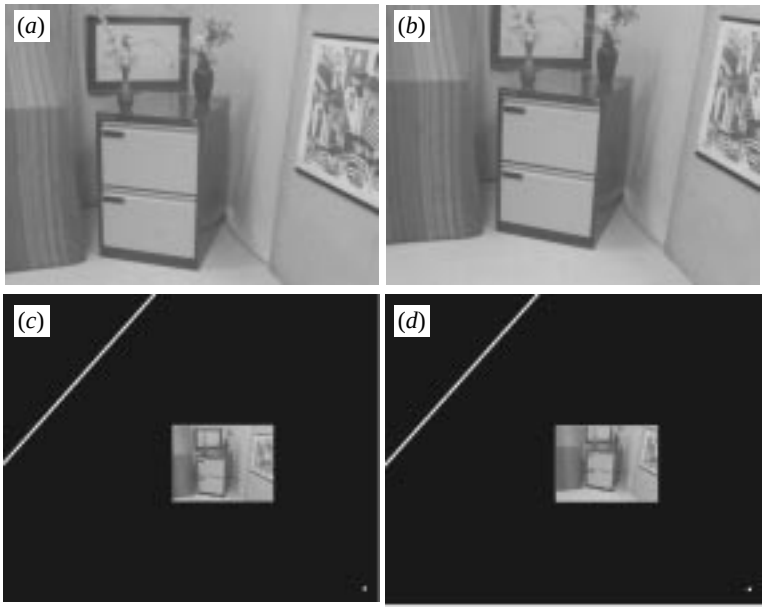


Figure 5. The motion between (*a*) and (*b*) is a rotation about the camera centre, with the rotation axis not aligned with with the image axes. (*c*) and (*d*) show the fixed point and line computed from the eigenvectors of $H_\infty$.

### (*c*) *Single motion of a fixed stereo rig*

Suppose a fixed stereo rig undergoes a general motion. Fixed here means that the relative orientation of the cameras on the rig is unchanged during the motion. The projective structure of the scene $\boldsymbol{X}$ can be obtained before ($\boldsymbol{X}_\mathrm{A}$) and after the motion ($\boldsymbol{X}_\mathrm{B}$). Since $\boldsymbol{X}_\mathrm{A}$ and $\boldsymbol{X}_\mathrm{B}$ are two projective reconstructions of the same scene, they are related by a $4 \times 4$ projective transformation $H_\mathrm{P}$, as $\boldsymbol{X}_\mathrm{B} = H_\mathrm{P}\boldsymbol{X}_\mathrm{A}$. It is shown in Zisserman *et al*. (1995) that since the actual motion of the rig is Euclidean, the homography $H_\mathrm{P}$ is conjugate to a Euclidean transformation, i.e. $H_\mathrm{P} = H_\mathrm{EP}^{-1}\, H_\mathrm{E}\, H_\mathrm{EP}$.

In Zisserman *et al*. (1995) an algorithm is described whereby the transformation $H_\mathrm{P}$ is computed automatically from 3D point reconstructions. The eigenvectors of $H_\mathrm{P}$ identify the fixed points and lines on $\boldsymbol{\pi}_\infty$, and thereby their images. An alternative parametrization of these results is given in Devernay & Faugeras (1996) and Horaud & Csurka (1998).

### (*d*) *Reconstruction ambiguity*

A particular family of solutions for $\boldsymbol{\omega}$ is often tightly coupled to a particular family of reconstructions. For the cases above (excluding the rotation about the camera centre for which 3D structure cannot be recovered), there is a one-parameter family of metric reconstructions.

Suppose, for ease of imagining, that the rotation axis is vertical. Since the circular points are known for planes orthogonal to the rotation axis, metric structure is known in horizontal planes. The only ambiguity remaining is an affine scaling in the vertical direction. The choice of this scaling corresponds to the one parameter in the $\boldsymbol{\omega}$ pencil.

Table 1. *Examples of commonly occurring rotations*

(These rotations fail to resolve the $\boldsymbol{\omega}$ ambiguity for various specified internal parameters (see the text for the comprehensive conditions). The rotation axis has direction $\boldsymbol{d}_r = (d_1, d_2, d_3)^T$. Rotations causing failure are indicated by X.)

| | parameter specified | | |
|---|---|---|---|
| axis of rotation | zero skew | principal point | aspect ratio |
| perpendicular to image plane, $\boldsymbol{d}_r = (0, 0, 1)^T$ | X | X | X |
| parallel to image plane, $\boldsymbol{d}_r = (*, *, 0)^T$ | | X | |
| parallel to the image $x$-axis, $\boldsymbol{d}_r = (1, 0, 0)^T$ | X | X | |
| parallel to the image $y$-axis, $\boldsymbol{d}_r = (0, 1, 0)^T$ | X | X | |

## 5. Resolving the ambiguity

In this section we answer the following question.

> Given the one-parameter family of solutions for $\boldsymbol{\omega}$ arising from a single rotation (3.3), when does an additional constraint *not* resolve the ambiguity?

The ambiguity is resolved once the value of $\mu$ in (3.3) is determined, since then the IAC, $\boldsymbol{\omega}$, (and equivalently the DIAC, $\boldsymbol{\omega}^*$), is uniquely determined. We will consider when this ambiguity is not resolved by placing constraints on the family by, for example, supplying values or ratios for particular internal parameters. The same constraint can be applied to both $\boldsymbol{\omega}$ and $\boldsymbol{\omega}^*$, but often the resulting (polynomial) equations are of lower complexity for one of them. The notation used here is that the rotation axis has direction $\boldsymbol{d}_r = (d_1, d_2, d_3)^T$. Table 1 summarizes the resolution ambiguities.

### (*a*) *Scene constraints*

We consider here the constraint imposed by the vanishing points of two orthogonal directions. Other orthogonality constraints, such as orthogonality between the vanishing line of a plane and the vanishing point of the normal direction to this plane, are applied in a similar manner.

Suppose the vanishing points of two orthogonal directions are $\boldsymbol{v}_1$ and $\boldsymbol{v}_2$, then from (2.3)

$$\boldsymbol{v}_1^T \boldsymbol{\omega} \boldsymbol{v}_2 = 0. \tag{5.1}$$

We seek the member of the pencil $C(\mu) = \boldsymbol{\Lambda}_2 + \mu\boldsymbol{\Lambda}_1$ which satisfies (5.1). This is a linear equation for $\mu$, namely $\boldsymbol{v}_1^T C(\mu)\boldsymbol{v}_2 = \boldsymbol{v}_1^T\boldsymbol{\Lambda}_2\boldsymbol{v}_2 + \mu\boldsymbol{v}_1^T\boldsymbol{\Lambda}_1\boldsymbol{v}_2 = 0$, and $\mu$ is determined uniquely provided $\boldsymbol{v}_1^T\boldsymbol{\Lambda}_1\boldsymbol{v}_2$ and $\boldsymbol{v}_1^T\boldsymbol{\Lambda}_2\boldsymbol{v}_2$ are non zero.

The alternative parametrization for $C(\mu) = \boldsymbol{\omega} + \mu\boldsymbol{\Lambda}_1$ illustrates why the ambiguity is not resolved. The IAC $\boldsymbol{\omega}$ obeys the constraint, and if also $\boldsymbol{v}_1^T\boldsymbol{\Lambda}_1\boldsymbol{v}_2 = 0$ (because $\boldsymbol{l}_r \cdot \boldsymbol{v}_1 = 0$ or $\boldsymbol{l}_r \cdot \boldsymbol{v}_2 = 0$), then all members of the family $C(\mu)$ satisfy the constraint, and consequently the value of $\mu$ cannot be determined. Since $\boldsymbol{\Lambda}_2$ is uniquely determined from $\boldsymbol{\omega}$ and $\boldsymbol{\Lambda}_1$, the necessary and sufficient condition for non-resolution is $\boldsymbol{v}_1^T\boldsymbol{\Lambda}_1\boldsymbol{v}_2 = (\boldsymbol{l}_r \cdot \boldsymbol{v}_1)(\boldsymbol{l}_r . \boldsymbol{v}_2) = 0$.

To summarize the argument of this subsection:

**Proposition 5.1.** *The ambiguity (3.3) cannot be resolved by an orthogonality constraint (5.1) if* $\boldsymbol{l}_\mathrm{r} \cdot \boldsymbol{v}_1 = 0$ *or* $\boldsymbol{l}_\mathrm{r} \cdot \boldsymbol{v}_2 = 0$.

This result can also be derived directly in terms of ray directions. Writing $\boldsymbol{l}_\mathrm{r} = A^{-\mathrm{T}}\boldsymbol{d}_\mathrm{r}$ and the image projections of the directions $\boldsymbol{v}_1 = A\boldsymbol{d}_1$ and $\boldsymbol{v}_2 = A\boldsymbol{d}_2$, then $(\boldsymbol{l}_\mathrm{r} \cdot \boldsymbol{v}_1)(\boldsymbol{l}_\mathrm{r} \cdot \boldsymbol{v}_2) = 0$ when

$$(\boldsymbol{l}_\mathrm{r} \cdot \boldsymbol{v}_1)(\boldsymbol{l}_\mathrm{r}.\boldsymbol{v}_2) = [(A^{-\mathrm{T}}\boldsymbol{d}_\mathrm{r})^\mathrm{T}(A\boldsymbol{d}_1)][(A^{-\mathrm{T}}\boldsymbol{d}_\mathrm{r})^\mathrm{T}(A\boldsymbol{d}_2)] = (\boldsymbol{d}_\mathrm{r}^\mathrm{T}\boldsymbol{d}_1)(\boldsymbol{d}_\mathrm{r}^\mathrm{T}\boldsymbol{d}_2) = 0. \quad (5.2)$$

That is, the constraint fails when the rotation axis direction is perpendicular to either of the line directions used to provide the orthogonality constraint.

For example, suppose the camera rotation is about a vertical world axis, then orthogonal vanishing points for directions in the horizontal world plane do not resolve the ambiguity. Note that this result applies for an arbitrary attitude of the camera.

### (*b*) *The skew-zero constraint*

This is the most commonly used additional constraint on the internal parameters. Its use has been suggested by several authors including Tomasi & Kanade (1992) and Luong & Viéville (1996).

In detail, we wish to impose the constraint that the image $x$ and $y$ axes are orthogonal. Orthogonality in the image is equivalent to conjugacy with respect to $\boldsymbol{\omega}$, so that two directions $\boldsymbol{v}_1$ and $\boldsymbol{v}_2$ are orthogonal if $\boldsymbol{v}_1^\mathrm{T}\boldsymbol{\omega}\boldsymbol{v}_2 = 0$. For the $x$ and $y$ axes $\boldsymbol{v}_1^\mathrm{T} = (1, 0, 0)$ and $\boldsymbol{v}_2^\mathrm{T} = (0, 1, 0)$, respectively, so that

$$(1, 0, 0)\boldsymbol{\omega}\begin{pmatrix}0\\1\\0\end{pmatrix} = 0. \quad (5.3)$$

It follows that $\boldsymbol{\omega}_{12} = \boldsymbol{\omega}_{21} = 0$.

As in the application of the orthogonal scene constraints above, the skew-zero constraint results in a linear equation for $\mu$. From proposition 5.1 the constraint does not resolve the ambiguity if $\boldsymbol{l}_\mathrm{r} \cdot \boldsymbol{v}_1 = 0$ or $\boldsymbol{l}_\mathrm{r} \cdot \boldsymbol{v}_2 = 0$. For example, suppose $\boldsymbol{l}_\mathrm{r} = (0, 1, -c)^\mathrm{T}$ (a horizontal line at $y = c$) which would result from a rotation about an axis parallel to the image $y$ axis. Then the pencil is

$$C(\mu) = \boldsymbol{\omega} + \mu\boldsymbol{l}_\mathrm{r}\boldsymbol{l}_\mathrm{r}^\mathrm{T} = \begin{bmatrix}* & 0 & *\\ 0 & * & *\\ * & * & *\end{bmatrix} + \mu\begin{bmatrix}0 & 0 & 0\\ 0 & * & *\\ 0 & * & *\end{bmatrix},$$

where $*$ indicates a non-zero element. Clearly all members of the pencil satisfy $\boldsymbol{\omega}_{12} = \boldsymbol{\omega}_{21} = 0$. Consequently, zero skew does *not* resolve the ambiguity.

From the direction formulation of (5.2) the ambiguity cannot be resolved if

$$\boldsymbol{d}_\mathrm{r} \cdot (1, 0, 0)^\mathrm{T} = 0 \quad \text{or} \quad \boldsymbol{d}_\mathrm{r} \cdot (0, 1, 0)^\mathrm{T} = 0,$$

i.e. if $d_1 = 0$ or $d_2 = 0$. For example, for the rotation parallel to the image $y$ axis of figure 4, $d_1 = 0$ and the ambiguity is not resolved. However, for the example of figure 5, where both $d_1 \neq 0$ and $d_2 \neq 0$, the ambiguity can be resolved.

The skew-zero constraint is one of the cases where there is a significant difference between placing a constraint on $\boldsymbol{\omega}$ or on $\boldsymbol{\omega}^*$. Imposing the constraint on $\boldsymbol{\omega}$ results in

a linear equation for $\mu$, whilst imposing the constraint on $\boldsymbol{\omega}^*$ results in a quadratic because the elements of $\boldsymbol{\omega}$ are quadratic polynomials (cofactors) in the elements of $\boldsymbol{\omega}^*$, and vice versa. Luong & Viéville (1996) imposed the constraint on the DIAC, and consequently obtained two solutions, one of which was fallacious and unnecessary.

### (*c*) *Specified principal point*

The principal point is the centre of $\boldsymbol{\omega}$. To see this, note that the centre, $\boldsymbol{c}$, of a conic $\mathsf{C}$ is the pole w.r.t. the line at infinity, $\boldsymbol{l}_\infty = (0,0,1)^{\mathrm{T}}$, i.e. $\boldsymbol{c} = \mathsf{C}^{-1}\boldsymbol{l}_\infty$. So in the case of $\boldsymbol{\omega}$,

$$\boldsymbol{c} = \boldsymbol{\omega}^{-1}\boldsymbol{l}_\infty = \boldsymbol{\omega}^*\boldsymbol{l}_\infty = (u_0, v_0, 1)^{\mathrm{T}}.$$

Consequently a specified principal point $\boldsymbol{p}^{\mathrm{T}} = (u_0, v_0, 1)$ places a pole–polar relationship on $\boldsymbol{\omega}^*$, namely $\boldsymbol{p} = \boldsymbol{\omega}^*\boldsymbol{l}_\infty$ (or equivalently on $\boldsymbol{\omega}$, i.e. $\boldsymbol{\omega}\boldsymbol{p} = \boldsymbol{l}_\infty$).

We first consider the case where the two components $(u_0, v_0)$ of the principal point are used to resolve the ambiguity. Note, this places two constraints on the one unknown parameter $\mu$.

The pencil of solutions for $\boldsymbol{\omega}^*$ can be written

$$\mathsf{C}^*(\lambda) = \boldsymbol{\omega}^* + \lambda \boldsymbol{v}_{\mathrm{r}}\boldsymbol{v}_{\mathrm{r}}^{\mathrm{T}}.$$

The centre of the dual of $\mathsf{C}^*(\lambda)$ is

$$\boldsymbol{c}(\lambda) = \mathsf{C}^*(\lambda)\boldsymbol{l}_\infty = \boldsymbol{\omega}^*\boldsymbol{l}_\infty + \lambda \boldsymbol{v}_{\mathrm{r}}\boldsymbol{v}_{\mathrm{r}}^{\mathrm{T}}\boldsymbol{l}_\infty = \boldsymbol{p} + \lambda \boldsymbol{v}_{\mathrm{r}}\boldsymbol{v}_{\mathrm{r}}^{\mathrm{T}}\boldsymbol{l}_\infty$$

since $\boldsymbol{\omega}^*\boldsymbol{l}_\infty = \boldsymbol{p}$. Consequently $\boldsymbol{c}(\lambda) = \boldsymbol{p}, \forall\lambda$ if (i) $\boldsymbol{v}_{\mathrm{r}} \cdot \boldsymbol{l}_\infty = 0$ or (ii) $\boldsymbol{v}_{\mathrm{r}} = \boldsymbol{p}$. Under these circumstances the entire pencil satisfies the constraint, and the ambiguity is not resolved. The directions for the two cases are:

1. $\boldsymbol{v}_{\mathrm{r}} \cdot \boldsymbol{l}_\infty = 0$. In this case $d_3 = 0$, which is a rotation with axis parallel to the image plane;

2. $\boldsymbol{v}_{\mathrm{r}} = \boldsymbol{p}$. In this case $\boldsymbol{d}_{\mathrm{r}} = \mathsf{A}^{-1}\boldsymbol{p}$, so that $d_1 = d_2 = 0$, which is a rotation with axis perpendicular to the image plane.

Since only one constraint in general is required to determine $\mu$, we now consider if there are additional ambiguities if only $u_0$ or $v_0$ are specified. Here $\boldsymbol{v}_{\mathrm{r}}$ is written as $\boldsymbol{v}_{\mathrm{r}} = (v_1, v_2, v_3)^{\mathrm{T}}$.

Specifying only $u_0$ we require that (i) $\boldsymbol{v}_{\mathrm{r}} \cdot \boldsymbol{l}_\infty = 0$ as before, but the second case reduces to (ii) $v_1/v_3 = u_0$. These conditions correspond to the direction constraints $d_3 = 0$ and $\alpha_u d_1 + k d_2 = 0$, respectively. Similarly, if only $v_0$ is specified (i) $\boldsymbol{v}_{\mathrm{r}} \cdot \boldsymbol{l}_\infty = 0$ as before, but the second case reduces to (ii) $v_2/v_3 = v_0$, and these conditions correspond to the directions $d_3 = 0$ and $d_2 = 0$, respectively.

To summarize for case (ii): specifying the principal point fails to resolve the ambiguity when the vanishing point of the axis of rotation coincides with the principal point (since all conics in the pencil will have the principal point as centre). Specifying one component of the principal point fails if that component of the vanishing point of the axis of rotation coincides with the corresponding component of the principal point.

### (*d*) *Specified aspect ratio*

We first obtain an expression for the aspect ratio of the calibration matrix $A(\mu)$ corresponding to a conic of the pencil $C(\mu)$. The matrix $A(\mu)$ is defined by $C(\mu) = (A(\mu)A(\mu)^{\mathrm{T}})^{-1} = A(\mu)^{-\mathrm{T}}A(\mu)^{-1}$. Writing the pencil $C(\mu) = \boldsymbol{\omega} + \mu \boldsymbol{l}_{\mathrm{r}}\boldsymbol{l}_{\mathrm{r}}^{\mathrm{T}}$ in terms of $A(0) = A$ (the true calibration matrix) and $\boldsymbol{d}_{\mathrm{r}}$,

$$\begin{aligned} C(\mu) &= A^{-\mathrm{T}}A^{-1} + \mu(A^{-\mathrm{T}}\boldsymbol{d}_{\mathrm{r}})(A^{-\mathrm{T}}\boldsymbol{d}_{\mathrm{r}})^{\mathrm{T}} \\ &= A^{-\mathrm{T}}(I + \mu \boldsymbol{d}_{\mathrm{r}}\boldsymbol{d}_{\mathrm{r}}^{\mathrm{T}})A^{-1} = A^{-\mathrm{T}}V(\mu)^{-\mathrm{T}}V(\mu)^{-1}A^{-1}, \end{aligned}$$

where $V(\mu)^{-\mathrm{T}}V(\mu)^{-1}$ is the Cholesky decomposition of $I + \mu \boldsymbol{d}_{\mathrm{r}}\boldsymbol{d}_{\mathrm{r}}^{\mathrm{T}}$, with $V(\mu)$ an upper triangular matrix. Thus $A(\mu)^{-\mathrm{T}} = A^{-\mathrm{T}}V(\mu)^{-\mathrm{T}}$. The results of the previous sections can also be derived from $A(\mu)$.

The aspect ratio $r(\mu)$ of $A(\mu)$ is obtained from the ratio of elements

$$A(\mu)_{22}^{-\mathrm{T}}/A(\mu)_{11}^{-\mathrm{T}}.$$

On examining

$$\begin{aligned} A(\mu)^{-\mathrm{T}} &= A^{-\mathrm{T}}V(\mu)^{-\mathrm{T}} \\ &= \begin{pmatrix} 1/\alpha_u & 0 & 0 \\ * & 1/\alpha_v & 0 \\ * & * & * \end{pmatrix} \begin{pmatrix} \sqrt{1+\mu d_1^2} & 0 & 0 \\ * & \sqrt{1+\mu d_2^2 - (\mu d_1 d_2)^2/(1+\mu d_1^2)} & 0 \\ * & * & * \end{pmatrix}, \end{aligned}$$

it is clear that the ratio $r(\mu)$ depends solely on $\alpha_u$, $\alpha_v$, $V_{11}$ and $V_{22}$, and is given by

$$r(\mu) = \frac{A(\mu)_{22}^{-\mathrm{T}}}{A(\mu)_{11}^{-\mathrm{T}}} = \frac{1}{\alpha_v}\sqrt{1+\mu d_2^2 - \frac{(\mu d_1 d_2)^2}{1+\mu d_1^2}} \Big/ \left(\frac{1}{\alpha_u}\sqrt{1+\mu d_1^2}\right). \tag{5.4}$$

We wish to impose the constraint that $r(\mu) = \alpha_u/\alpha_v$ in order to resolve the ambiguity. Applying this equality to (5.4) gives

$$\mu(d_1^4\mu + d_1^2 - d_2^2) = 0. \tag{5.5}$$

It follows that if $d_1 = d_2 = 0$ then the constraint is satisfied for all values of $\mu$. Conversely if $d_1 = d_2 = 0$, then applying the constraint does not determine $\mu$, and so does not resolve the ambiguity.

Note, in general two values of $\mu$, and thus two conics in the pencil, satisfy the aspect ratio constraint. For the parametrization $C(\mu) = \boldsymbol{\omega} + \mu \boldsymbol{l}_{\mathrm{r}}\boldsymbol{l}_{\mathrm{r}}^{\mathrm{T}}$ the conic corresponding to $\mu = 0$ is the true solution, $\boldsymbol{\omega}$, and the other is spurious.

## 6. Discussion

Often when there is a family of solutions (for $\boldsymbol{\omega}$ say) further constraints are added to resolve the ambiguity. These constraints may be *consistent* (i.e. already satisfied by the family), or *complementary*, i.e. the additional constraints do reduce the ambiguity. Unfortunately as measurements contain errors, consistent constraints can be mistaken for complementary ones, and the ambiguity is then resolved by the noise. In the case of motions which are close to critical motion sequences this resolution will be very poorly conditioned. Further details are given in Armstrong (1996).

Clearly it is important to identify poorly conditioned solutions under such circumstances and this requires, at the very least, that auto-calibration algorithms also compute an uncertainty for the estimated metric calibration.

This paper has examined whether constraints are complementary or consistent for one type of critical motion sequence. The other types of motion ambiguity described in Sturm (1997) can be examined in a similar manner.

We are grateful for comments from Marc Pollefeys and Lourdes de Agapito, and for financial support from Esprit Project Improofs.

## References

Armstrong, M. 1996 Self-calibration from image sequences. Ph.D. thesis, University of Oxford, UK.

Armstrong, M., Zisserman, A. & Beardsley, P. 1994 Euclidean reconstruction from uncalibrated images. In *Proc. British Machine Vision Conf.*, pp. 509–518.

Armstrong, M., Zisserman, A. & Hartley, R. 1996 Self-calibration from image triplets. In *Proc. European Conf. on Computer Vision*. Lecture Notes in Computer Science, vol. 1064/1065, pp. 3–16. Springer.

Beardsley, P. & Zisserman, A. 1995 Affine calibration of mobile vehicles. In *Europe-China workshop on Geometrical Modelling and Invariants for Computer Vision* (ed. R. Mohr & W. Chengke), pp. 214–221. Xi'an, China: Xidan University Press.

Beardsley, P., Torr, P. & Zisserman, A. 1996 3D model acquisition from extended image sequences. In *Proc. European Conf. on Computer Vision*. Lecture Notes in Computer Science, vol. 1064/1065, pp. 683–695. Springer.

Bougnoux, S. 1998 From Projective to Euclidean space under any practical situation, a criticism of self-calibration. In *Proc. 6th Int. Conf. on Computer Vision, Bombay*, pp. 790–796.

Devernay, F. & Faugeras, O. 1996 From projective to Euclidean reconstruction. In *Proc. Computer Vision and Pattern Recognition*, pp. 264–269.

Faugeras, O. 1993 *Three-dimensional computer vision: a geometric viewpoint*. MIT Press.

Faugeras, O. 1995 Stratification of three-dimensional vision: projective, affine, and metric representation. *J. Opt. Soc. Am.* A **12**, 465–484.

Faugeras, O., Luong, Q. & Maybank, S. 1992 Camera self-calibration: theory and experiments. In *Proc. European Conf. on Computer Vision*. Lecture Notes in Computer Science, vol. 588, pp. 321–334. Springer.

Hartley, R. 1992 Estimation of relative camera positions for uncalibrated cameras. In *Proc. European Conf. on Computer Vision*. Lecture Notes in Computer Science, vol. 588, pp. 579–587. Springer.

Hartley, R. 1994*a* Euclidean reconstruction from uncalibrated views. In *Applications of invariance in computer vision* (ed. J. Mundy, A. Zisserman & D. Forsyth), pp. 237–256. Lecture Notes in Computer Science, vol. 825. Springer.

Hartley, R. 1994*b* Self-calibration from multiple views with a rotating camera. In *Proc. European Conf. on Computer Vision*. Lecture Notes in Computer Science, vol. 800/801, pp. 471–478. Springer.

Hartley R. 1995 A linear method for reconstruction from lines and points. In *Proc. Int. Conf. on Computer Vision*, pp. 882–887.

Heyden, A. & Åström, K. 1997 Euclidean reconstruction from image sequences with varying and unknown focal length and principal point. In *Proc. Computer Vision and Pattern Recognition*.

Horaud, R. & Csurka, G. 1998 Self-calibration and Euclidean reconstruction using motions of a stereo rig. In *Proc. 6th Int. Conf. on Computer Vision, Bombay*, pp. 96–103.

Kanatani, K. 1992 *Geometric computation for machine vision*. Oxford University Press.

Laveau, S. 1996 Geometry of a system of $N$ cameras. Theory, estimation, and applications. Ph.D. thesis, INRIA.

Luong, Q. 1992 Matrice fondamentale et autocalibration en vision par ordinateur. Ph.D. thesis, Université de Paris-Sud, France.

Luong, Q. & Viéville, T. 1994 Canonic representations for the geometries of multiple projective views. In *Proc. 3rd European Conf. on Computer Vision, Stockholm*, pp. 589–599.

Luong, Q. & Viéville, T. 1996 Canonical representations for the geometries of multiple projective views. *Computer Vision Image Understanding* **64**, 193–229.

Mundy, J. & Zisserman, A. 1992 *Geometric invariance in computer vision*. MIT Press.

Pollefeys, M., Van Gool, L. & Proesmans, M. 1996 Euclidean 3D reconstruction from image sequences with variable focal lengths. In *Proc. European Conf. on Computer Vision*. Lecture Notes in Computer Science, vol. 1064/1065, pp. 31–42. Springer.

Pollefeys, M., Koch, R. & Van Gool, L. 1998 Self calibration and metric reconstruction in spite of varying and unknown internal camera parameters. In *Proc. 6th Int. Conf. on Computer Vision, Bombay*, pp. 90–95.

Semple, J. & Kneebone, G. 1979 *Algebraic projective geometry*. Oxford University Press.

Sturm, P. 1997 Critical motion sequences for monocular self-calibration and uncalibrated Euclidean reconstruction. In *Proc. Conf. on Computer Vision and Pattern Recognition, Puerto Rico*, pp. 1100–1105.

Tomasi, C. & Kanade, T. 1992 Shape and motion from image streams under orthography: a factorization approach. *Int. J. Computer Vision* **9**, 137–154.

Triggs, B. 1997 Auto-calibration and the absolute quadric. In *Proc. Conf. on Computer Vision and Pattern Recognition, Puerto Rico*, pp. 609–614.

Zeller, C. 1996 Projective, affine and Euclidean calibration in computer vision and the application of three dimensional perception. Ph.D. thesis, RobotVis Group, INRIA Sophia-Antipolis.

Zisserman, A., Beardsley, P. & Reid, I. 1995 Metric calibration of a stereo rig. In *IEEE Workshop on Representation of Visual Scenes, Boston*, pp. 93–100.

## *Discussion*

O. Faugeras (*INRIA, France*). My first question is about the ambiguity that was in the work of Luong & Viéville because they looked at the wrong (the dual) conic. What is the interpretation of the second solution?

A. Zisserman. I don't have a geometric interpretation, but algebraically the second solution arises because elements of the dual conic are cofactors, and therefore quadratic in the elements of the original conic. A linear condition on the original conic (the image of the absolute conic) becomes quadratic when applied to the dual conic, and hence there are two solutions. I think the second solution is just fallacious.

O. Faugeras. My second question is, in the calibration of the stereo rig, the 3D collineation is estimated to have magnitude one eigenvalues; are these constraints enforced in the estimation, and if not would it help?

A. Zisserman. No, we didn't enforce the constraints. The collineation was computed from hundreds of point correspondences, so in terms of an estimation problem it was very well constrained. The estimated matrix closely approximated the correct algebraic structure. However, I think it would be better to impose the constraints during the minimization so that the estimated matrix had exactly the correct algebraic structure.

R. I. Hartley (*GE Corporate Research and Development, Niskayuna, NY, USA*). When the individual projective reconstructions are constructed, are all the points

put in together from both views to construct the fundamental matrix? Because you start with a stereo rig, with a fundamental matrix, you move the rig, but you've got the same fundamental matrix. You could throw all the points in from both stereo pairs.

A. Zisserman. I know, but we didn't, because again, as we had hundreds of correspondences automatically computed, the estimated fundamental matrix was extremely good. But Dr Hartley is quite right, we could have combined them all.

R. I. Hartley. To estimate the projective transformation what did Dr Zisserman minimize?

A. Zisserman. We minimized reprojection error. Minimizing errors in three dimensions produces inferior results.

T. Kanade (*Robotics Institute, Carnegie Mellon University, Pittsburgh, PA, USA*). Simple question. How does Dr Zisserman deal with radial distortion—before or after?

A. Zisserman. What we've tended to do is try to ignore it if we can; if the camera lenses are of sufficient quality, without significant radial distortion, then we don't do anything about it. The multiple-view relations are very forgiving of radial distortion. When the radial distortion is significant we compute a radial correction in advance and map the points so that the camera model is effectively linear; only the features are mapped, it is not necessary to warp the image.

T. Kanade. Does that mean that he has to do camera's internal calibration?

A. Zisserman. I guessed that was coming. It is necessary to make assumptions in order to compute radial correction. For example, that the centre of radial distortion is near to the centre of the image, and some assumption about the aspect ratio, but that's all we need to bring in. Devernay & Faugeras (1995) describe a method which solves for these parameters and the first-order radial correction based on straight lines in the scene. But as I said, most of the time we do not have to make a radial correction because with the camera lenses we're using it's not a problem. With a lens like that of the SGI IndyCam, of course, a correction has to be made.

J. L. Mundy (*GE Corporate Research and Development, Niskayuna, NY, USA*). It seems as though Dr Zisserman has done quite a large number of experiments and has observed a lot of different situations and types of objects and so forth. Does he have any feeling at this point whether points or lines are more robust in their ability to produce structure? Would he have any preference between points and lines now, based on his experience?

A. Zisserman. Lines are still the weaker of the two for several reasons. First, when we compute multiple-view relations, such as the trifocal tensor, we generally compute the initial estimate using points because fewer correspondences are required than for lines (six-point correspondences compared to nine-line correspondences). The smaller size for the minimal set is important when obtaining samples for the RANSAC robust estimator. Second, line matching is not so successful without the constraints provided by the multiple-view relations. So we tend to estimate the trifocal tensor, for example, using point correspondences, and then use this tensor to guide line matching. Third, with three-dimensional structure recovery, there are problems with lines when they lie near to epipolar planes. Points do not suffer from this degeneracy. We estimate

the final structure by bundle adjusting both points and lines over multiple views (minimizing the reprojection error). Even so, occasional 3D lines are still in error because of these degeneracies in line reconstruction. On the other hand, lines are much more informative visually than points because they give a better impression of the three-dimensional structure and its connectivity.

W. Triggs (*INRIA, France*). What about using more dense forms of structure than points and lines?

A. Zisserman. Such as dense correspondences? Yes, we're definitely going to move onto that, but using the matched points and lines to guide the dense correspondence. We've now got excellent multiple-view relations, so we don't have to do dense correspondence and search in a correlation window over the image. Instead we can search along epipolar lines and verify using trifocal or other multiple-view relations.

W. Triggs. And how much will this buy in terms of accuracy?

A. Zisserman. It's for visualization rather than accuracy. The points and the lines give very accurate multiple-view relations. With dense correspondences the advantage is in being able to reconstruct surfaces where there are no corner and line features.

*Additional references*

Devernay, F. & Faugeras, O. 1995 Automatic calibration and removal of distortion from scenes of structured environments. Society of Photo-Optical Instrumentation Engineers.





PHILOSOPHICAL TRANSACTIONS OF THE ROYAL SOCIETY A MATHEMATICAL, PHYSICAL & ENGINEERING SCIENCES

PHILOSOPHICAL TRANSACTIONS OF THE ROYAL SOCIETY A MATHEMATICAL, PHYSICAL & ENGINEERING SCIENCES